

## Molecular self-diffusion and micellar structure in the aqueous solutions of AF9-10 ethoxylated isononylphenol near a cloud point

Victor P. Arkhipov,<sup>a</sup> Zamil Sh. Idiyatullin,<sup>a</sup> Oleg I. Gnezdilov,<sup>b</sup>  
Ekaterina V. Petrova,<sup>a</sup> Andrey V. Filippov<sup>\*b,c</sup> and Oleg N. Antzutkin<sup>c,d</sup>

<sup>a</sup> Kazan National Research Technological University, 420015 Kazan, Russian Federation

<sup>b</sup> Institute of Physics, Kazan (Volga Region) Federal University, 420008 Kazan, Russian Federation.

Fax: +7 843 231 5189; e-mail: [Andrey.Filippov@kpfu.ru](mailto:Andrey.Filippov@kpfu.ru)

<sup>c</sup> Chemistry of Interfaces, Luleå University of Technology, SE-91187 Luleå, Sweden

<sup>d</sup> Department of Physics, Warwick University, CV4 7AL Coventry, UK

DOI: 10.1016/j.mencom.2014.09.006

Sizes of micelles and compositions of aggregates in the aqueous solutions of the nonionic surfactant oxyethylated monoalkyl phenol (neonol AF9-10) were determined by NMR spectroscopy, NMR diffusometry and dynamic light scattering in a wide range of temperatures near the cloud point. The cloud point extraction of phenol from aqueous solutions by the surfactant AF9-10 was performed.

In the aqueous solutions of nonionic surfactants, turbidity is observed with increasing temperature due to a phase transition from uniform micelles to nonuniform biphasic solution consisting of a surfactant-depleted phase and a surfactant-rich phase.<sup>1</sup> The turbidity or cloud of the solution results from light scattering by density fluctuations formed by irregular surfactant aggregates, whose dimensions are comparable to wavelengths in the visible range.

An increase in surfactant concentrations leads to a change in the micelle shape from spherical to rod-like. The core of micelles is formed by hydrophobic hydrocarbon tails, while hydrophilic polar oxyethylene chains form a thick extensive surface of micelles. The micelles contain water associated with oxygen of surfactant oxyethylene groups through hydrogen bonds. The cloud phenomenon is explained by the dehydration of oxyethylene chains under increasing temperature and by the formation of aggregates (clusters) of dehydrated surfactant molecules, which have low solubility in water and are prone to sedimentation. Changes in the surfactant properties with cloud point (CP) transition are used in a cloud point extraction (CPE) method, which is applied to extract hydrophobic organic compounds such as phenols and polycyclic aromatic hydrocarbons.<sup>2,3</sup> The aim of this work was to study the properties of nonionic surfactants near the CP using aqueous solutions of oxyethylated monoalkyl phenol (neonol AF9-10). Neonol AF9-10 is a water-soluble high-effective nonionic surfactant. The CP of an aqueous solution of AF9-10 with concentration 10 g dm<sup>-3</sup> is 66±3 °C. We used NMR diffusometry, NMR spectroscopy and dynamic light scattering at a constant AF9-10 concentration of 10 g dm<sup>-3</sup> in a temperature range of 30–90 °C. This temperature range covers the region of existence of micellar solution, the transition region near the CP and the region of two-phase solution containing aggregates of surfactant molecules. Removal of phenol from aqueous solutions by the CPE method using AF9-10 was analyzed.<sup>†</sup>

Neonol solutions were transparent below the cloud point, while they were bluish-white above it. Therefore, it is believed that micelle sizes below the CP did not exceed 50 nm, and

aggregates or clusters formed above the CP had dimensions of 100–1000 nm.

In the study of fast processes or thermal studies, one should take into account the rate of relaxation processes of nuclear magnetization, the spin–spin and spin–lattice relaxation. We measured the integrated intensities of the protons of water and surfactant oxyethylene groups in <sup>1</sup>H NMR spectra<sup>‡</sup> to understand what changes occur in micelle composition near the cloud point. To minimize the error of integration of closely spaced lines, two kinds of solutions were prepared: in ordinary water H<sub>2</sub>O and in deuterated water D<sub>2</sub>O, and accordingly, two series of measurements were carried out. In the H<sub>2</sub>O solutions, the integrated intensities of water lines were measured, while the contributions of oxyethylene protons could be neglected because of a low surfactant concentration. In the D<sub>2</sub>O solutions, we measured the integrated intensity of surfactant oxyethylene protons; in this case, the contribution of deuterated water residual protons was negligible.

To avoid distortion of the integrated intensities in the NMR spectra due to a saturation phenomenon, rest time was chosen ≈ 5T<sub>1</sub> (T<sub>1</sub> is the spin–lattice relaxation time). Relaxation times T<sub>1</sub> measured by the two-pulse sequence 180°–τ–90° with increasing temperature from 30 to 90 °C ranged within 1.9–2.8 and 5–20 s for water protons and residual protons of deuterated water, respectively. The relaxation times of oxyethylene protons in all solutions did not exceed 1 s. The integrated intensities were compared with each other considering the temperature dependence of the magnetic susceptibility (Curie law) and water density.

Selective measurements of self-diffusion coefficients (SDCs) of water and surfactant molecules were carried out by an NMR spin echo technique with a pulsed magnetic field gradient.<sup>‡,4</sup> The maximum amplitude of a pulsed magnetic field gradient was 0.5 T m<sup>-1</sup>. The Fourier transformation of the echo signal allowed us to obtain in one experiment the SDCs of different molecules characterized by distinct NMR chemical shifts.<sup>5,6</sup> We experimentally estimated surfactant SDCs using diffusion decays of the signal of oxyethylene protons (4.0 ppm), while SDCs of water molecules were determined from diffusion decay

<sup>†</sup> Commercial AF9-10 [C<sub>9</sub>H<sub>19</sub>C<sub>6</sub>H<sub>4</sub>O(C<sub>2</sub>H<sub>4</sub>O)<sub>10</sub>H] from Nizhnekamsk-neftekhim (Russia, [www.elarum.ru/standarts/tu-2483-077-05766801-98](http://www.elarum.ru/standarts/tu-2483-077-05766801-98)) was used without further purification. Chemically pure phenol (Sigma), deionized water and deuterated water (99%, Sigma) were used to prepare solutions.

<sup>‡</sup> The NMR spectra were recorded using Tesla-BS567A (<sup>1</sup>H, 100 MHz) and Bruker Avance 400 WB (<sup>1</sup>H, 400 MHz) spectrometers. The measurements of SDCs were performed using a Tesla-BS567A spectrometer equipped with a pulsed gradient unit.

of the signal of hydroxyl protons (4.7 ppm). SDC estimation error did not exceed 3%. The hydrodynamic radii of micelles were calculated assuming a spherical shape of micelles, which is quite adequate for a low surfactant concentration. Both methods are based on the hydrodynamic Stokes–Einstein relation

$$D = \frac{kT}{6\pi\eta R}, \quad (1)$$

where  $k$  is the Boltzmann constant,  $T$  is the temperature,  $\eta$  is the solvent viscosity,  $R$  is the radius, and  $D$  is the SDCs of micelles or aggregates, respectively. Surfactant SDCs ( $D_s$ ) are an effective weight average of all possible states of surfactant molecules in solution. In the two-state model,<sup>7</sup> the monomolecular and micelle states of a surfactant in solution are considered; therefore,  $D_s$  is the sum of the two components

$$D_s = \frac{\text{CMC}}{C} D_s^{\text{free}} + \frac{C - \text{CMC}}{C} D_s^{\text{bound}}, \quad (2)$$

where  $D_s^{\text{free}}$  and  $D_s^{\text{bound}}$  are SDCs of individual molecules and surfactant micelles, respectively;  $C$  is the surfactant concentration in solution; and CMC is the critical micelle concentration. The concentration of free surfactant molecules in solution at  $C > \text{CMC}$  is equal to CMC.<sup>7</sup>  $D_s^{\text{free}}$  is calculated from the value of  $D_s$  at  $C = \text{CMC}$  taking into account the hindering influence of micelles:

$$D_s^{\text{free}} = \frac{D_s^{\text{CMC}}}{1 + \phi/2}, \quad (3)$$

where  $\phi$  is the volume content of micelles, which can be estimated from known molecular masses  $\mu$ , densities  $\rho$  and CMC of AF9-10:<sup>8</sup>

$$\phi = \frac{(C - \text{CMC})\mu}{\rho}. \quad (4)$$

The dynamic light scattering (DLS) measurements were performed using a Zetasizer Nano-ZS instrument, equipped with a He–Ne laser,  $\lambda = 632.8$  nm. Micelles or aggregates mobility was estimated by analysis of the time correlation function of fluctuations in frequency, intensity and direction of scattered light, and then their sizes were automatically calculated with equation (1).

Figure 1 shows the normalized integrated intensities of water and surfactant oxyethylene protons in the NMR spectra of AF9-10 aqueous solution ( $C_{\text{surf}} = 10 \text{ g dm}^{-3}$ ) vs. temperature. The integrated intensity of water protons exhibited no significant difference under temperature variation (below, near and above the CP). In the solution with surfactant concentration of  $66 \text{ g dm}^{-3}$ , the integral intensity of water protons also did not vary with temperature. At the same time, the integrated intensity of surfactant oxyethylene protons did not change until the CP temperature was reached and then sharply decreased. According to our calcula-

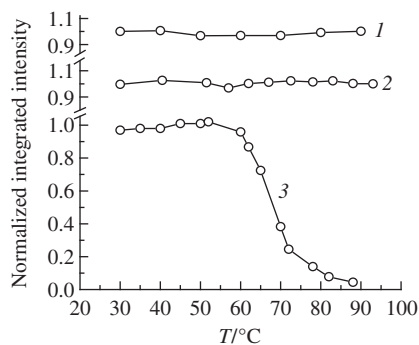


**Figure 1** Normalized integrated intensities of the proton NMR lines in aqueous AF9-10 solutions: (1) water ( $C_{\text{surf}} = 66 \text{ g dm}^{-3}$ ), (2) water and (3) surfactant oxyethylene groups ( $C_{\text{surf}} = 10 \text{ g dm}^{-3}$ ).

tions, the surfactant concentration in the solution above the CP was close to the CMC.

Clearly, there is a homogeneous micellar aqueous surfactant solution below CP. Due to high mobility of all solution components, the NMR spectral lines of water and surfactant are narrow and their integrated intensities are kept constant. The sharp decrease in the intensities of surfactant spectral lines above CP is derived from two reasons. The first one is dehydration of oxyethylene groups of surfactant molecules and the formation of aggregates of these dehydrated molecules. Although aggregate sizes are about 100–1000 nm, this does not change the integral intensities of the surfactant spectral lines, leading only to their slight broadening.<sup>9,10</sup> The second reason is the sedimentation of surfactant aggregates. Due to destruction of hydrogen bonds with water molecules, the solubility of surfactant decreases. Because of sedimentation, the spatial separation of surfactant-rich and a surfactant-depleted phases takes place. Surfactant-rich phase forms a layer on the top of the sample located outside the NMR measuring head. Solution with a surfactant-depleted phase occupies the rest of the sample volume that is already within the sensitive area of the NMR probe. Thus, the observed NMR signal will contain contributions of surfactant protons in surfactant-depleted phase only. Phase separation is fast enough within 10–15 min, and the surfactant concentration in the surfactant-depleted phase is determined by temperature.

Figure 2 shows the results of selective SDCs measurements of water and surfactant molecules in aqueous solutions. Within experimental error, the temperature dependence of water molecules SDCs was linear and monotonic over the entire temperature range. The observed SDCs of water in solutions are lower than that of neat water because of aggregate obstruction and surfactant hydration.<sup>11</sup> The SDCs of surfactant molecules also change monotonically with temperature up to the CP. The SDCs measurements above the CP had a large error due to low concentration (equal to CMC) of surfactant in the aqueous phase. Measurements of SDCs of surfactant aggregates forming a surfactant-rich phase were beyond the capabilities of the NMR method.

The temperature dependence of water and surfactants SDCs in the Arrhenius coordinates had an opposite appearance. The SDCs of water molecules increased with temperature with an activation energy of about  $15.3 \text{ kJ mol}^{-1}$ . At the same time, the SDCs of surfactant molecules decreased with temperature; the apparent activation energy was  $-9.8 \text{ kJ mol}^{-1}$ . The negative activation energy of surfactant diffusion can be related to structural changes occurring in the solution. The decrease of surfactant SDCs with temperature is due to growing sizes of surfactant micelles and aggregates.<sup>12</sup>

Using water and surfactant SDCs provided by NMR, we evaluated the diameters of surfactant micelles (Figure 3). There was a good agreement between micelle diameters obtained by NMR and DLS methods in the micellar region below the CP tem-

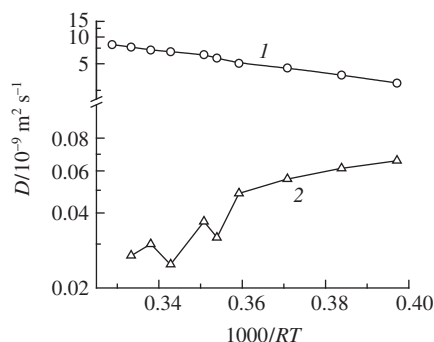


**Figure 2** Self-diffusion coefficients in aqueous AF9-10 solution ( $C_{\text{surf}} = 10 \text{ g dm}^{-3}$ ): (1) water and (2) surfactant.

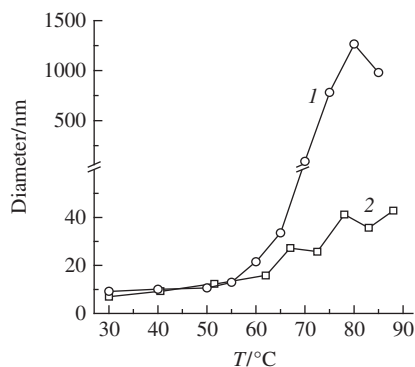


**Figure 3** Diameters of surfactant micelles and aggregates in aqueous AF9-10 solution ( $C_{\text{surf}} = 10 \text{ g dm}^{-3}$ ) obtained by (1) DLS and (2) NMR diffusometry.

perature. Moreover, DLS was complementary to NMR method to determine the sizes of aggregates above the CP.

DLS allowed us to see the dynamics of change in the size of micelles in surfactant solution under increasing temperature. The results obtained by DLS at temperatures below, near and above the CP are shown in Figure S1 (Online Supplementary Materials). Below the CP, the surfactant existed mainly in the micellar form with an average micelle diameter of 20–25 nm. Above the CP, it formed aggregates with an average diameter of ~500 nm. Solution in the transition region near the CP contained both the micelles and aggregates of surfactant molecules.

Phenol is a well-known environmental toxicant.<sup>13,14</sup> Below we consider the possibility of phenol extraction from aqueous solutions using the CPE method and AF9-10 as a surfactant. The efficiency and dynamics of phenol extraction can be controlled by changes in the integrated intensities of its lines in NMR spectrum.

Since phenol extracted by CPE is transferred to a surfactant-rich phase, further phase separation occurs and as a result of sedimentation the surfactant-rich phase with phenol collects in the upper part of the sample. The lower portion of the sample represents a surfactant-depleted phase almost free of phenol. The efficiency of the extraction process can be estimated by changes in the concentration of phenol at the bottom of the sample compared with its initial concentration.

The proton spectral lines of phenol and phenyl surfactant groups are overlapping. According to the numbers of phenyl (4), alkyl (19) and oxyethylene (40) protons in the AF9-10 molecule and the integrated intensities of surfactant alkyl  $I_{\text{alk}}$  and  $I_{\text{eth}}$  oxyethylene protons in a spectrum, the contribution of the phenol protons  $I_{\text{ph}}$  to the resulting integrated intensity in the aromatic region  $I_{\Sigma}$  was determined:

$$I_{\text{ph}} = I_{\Sigma} - 2(I_{\text{alk}}/19 + I_{\text{eth}}/40). \quad (5)$$

Change in the integrated intensity of phenol protons during the CPE process was monitored relative to the line of residual water protons. As shown above, the integrated intensity of the water proton line does not vary with temperature. The extraction efficiency  $E$  was determined by a standard procedure:<sup>3</sup>

$$E = \frac{I_{\text{ph},0} - I_{\text{ph}}}{I_{\text{ph},0}}, \quad (6)$$

where  $I_{\text{ph},0}$  and  $I_{\text{ph}}$  are the integrated intensities of a phenol line in the lower part of the sample at the beginning of and during the extraction process, respectively.

Usual procedure for CPE efficiency evaluation requires centrifugation, and then the concentration of recoverable reagent is

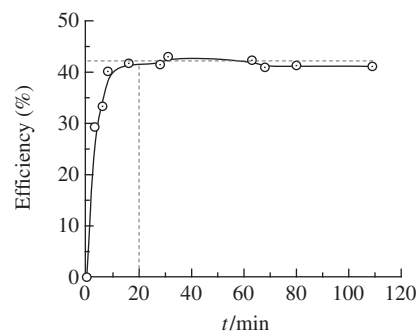


**Figure 4** Efficiency of phenol extraction from aqueous solutions.  $C_{\text{surf}} = 66 \text{ g dm}^{-3}$ ; initial phenol concentration,  $4.7 \text{ g dm}^{-3}$ .

determined by spectroscopy or liquid chromatography. The NMR method makes it possible to determine the CPE efficiency in time directly in the test sample without any influence on it. Experimental results of time dependence study of the efficiency of phenol extraction from aqueous solutions using the surfactant AF9-10 are shown in Figure 4. The extraction was almost complete after 20 min. Similar data were obtained for CPE of phenol from aqueous solutions by PONPE10<sup>3</sup> and Triton X-114.<sup>15</sup>

Test measurements of the efficiency of phenol CPE from aqueous solutions using AF9-10 were performed at varying surfactant and phenol concentrations. The average extraction efficiency was about 43%, which is in a good agreement with the data<sup>3</sup> for the CPE of phenol from aqueous solutions using a similar surfactant PONPE10. Thus, the CP extraction of phenol from aqueous solutions can be carried out using AF9-10 as a surfactant.

#### Online Supplementary Materials

Supplementary data associated with this article can be found in the online version at doi:10.1016/j.mencom.2014.09.006.

#### References

- 1 K. Holmberg, B. Jönsson, B. Kronberg and B. Lindman, in *Surfactants and Polymers in Aqueous Solution*, 2<sup>nd</sup> edn., John Wiley & Sons, Ltd., 2003.
- 2 W. L. Hinze, in *UNC-WRRI*, 269, Water Resources Institute of the University of North Carolina, 1992.
- 3 S. Akita and H. Takeuchi, *Sep. Sci. Technol.*, 1995, **30**, 833.
- 4 V. D. Fedotov, Yu. F. Zuev, V. P. Archipov and Z. Sh. Idrayatullin, *Appl. Magn. Reson.*, 1996, **11**, 7.
- 5 T. L. James and G. G. McDonald, *J. Magn. Reson.*, 1973, **11**, 58.
- 6 V. P. Archipov, E. F. Potapova, O. N. Antzutkin and A. V. Filippov, *Magn. Reson. Chem.*, 2013, **51**, 424.
- 7 *Microemulsions: Structure and Dynamics*, eds. S. E. Friberg and P. Bothorel, CRC Press, Inc., Boca Raton, 1988.
- 8 A. Tihova, N. Gluhareva and E. Kolesnikova, *Sci. Stat. BelsU, Ser. Nat. Sci.*, 2010, **21**, 127.
- 9 A. Filippov, A. Khakimov, S. Afonin and O. N. Antzutkin, *Mendeleev Commun.*, 2013, **23**, 313.
- 10 J. Spevacek, L. Hanykova and L. Starovoytova, *Macromolecules*, 2004, **37**, 7710.
- 11 P. G. Nilsson and B. Lindman, *J. Phys. Chem.*, 1983, **87**, 4756.
- 12 B. Wyn, R. Johnsen, P. Stilbs and B. Lindman, *J. Phys. Chem.*, 1983, **87**, 4548.
- 13 V. N. Bekhterev and E. A. Kabina, *Mendeleev Commun.*, 2007, **17**, 45.
- 14 N. A. Penner, P. N. Nesterenko, A. V. Khryashevsky, T. N. Stranadko and O. A. Shpigun, *Mendeleev Commun.*, 1998, 24.
- 15 E. Katsoyannos, A. Chatzilazarou, O. Gortzi, S. Lalas, S. Konteles and P. Tataridis, *Fresenius Environ. Bull.*, 2006, **15**, 1122.

Received: 25th November 2013; Com. 13/4250